Int. J. Electrochem. Sci., 16 **(2021)** Article ID: 210626, doi: 10.20964/2021.06.29

International Journal of ELECTROCHEMICAL SCIENCE
www.electrochemsci.org

Short Communication

Synergistic inhibition effect of Polyacrylamide and Tetradecylpyridinium bromide on corrosion behavior of carbon steel rebar in simulated cement-mortar pore solution

Ruo-li Shi[1], *Jun Zhang*[1,*], *Shao-hua Shi*[2]

[1] School of Architecture and Planning, Yunnan University, Kunming 650091, Yunnan, China
[2] School of Architectural Engineering, Sichuan University of Arts and Science, Dazhou, Sichuan Province, 635000, China
[*]E-mail: zhangj00101@sina.com

Received: 1 February 2021 / *Accepted:* 30 March 2021 / *Published:* 30 April 2021

Synergistic inhibition effect of Polyacrylamide (PA) and Tetradecylpyridinium bromide (TTAB) on the corrosion behavior of carbon steel rebar in simulated cement-mortar pore solution was evaluated by electrochemical impedance spectroscopy (EIS) and potentiodynamic polarization techniques. The EIS results revealed that the PA as a mixed-type inhibitor considerably enhanced corrosion protection performance in carbon steel rebar with creation of an organic layer to prevent both cathodic and anodic corrosion reactions. The obtained electrochemical results show that the inhibition efficiency of PA was significantly enhanced in the presence of TTAB for carbon steel rebar which confirms the synergistic corrosion effect between TTAB and PA. Because the inhibitor type changed from mixed-type to anodic-type through the increase of TTAB concentration, they eventually delayed the anodic dissolution of carbon steel which reduced the corrosion rate of the steel rebar in an aggressive environment.

Keywords: Synergistic inhibition effect; Corrosion resistance; Simulated cement-mortar pore solution; Electrochemical methods

1. INTRODUCTION

Nowadays, steel and related alloys have a fundamental role in social advancement because of excellent mechanical strength, facile fabrication, and their merits on cost effectiveness [1-3]. Application-specific necessities for advanced steel types include continuous stability in ambient media such as aggressive solutions for steel reinforced concrete structures and oil pipelines [4-6], allowing for predictable topics on the corrosion.

Using inhibitors are one of most practical techniques for protecting metals against corrosion, particularly in an alkaline environment [7, 8]. Most familiar inhibitors are organic compounds

including oxygen, sulfur, and nitrogen atoms [9]. Among them, the surfactant inhibitors have many benefits such as easy production, high inhibition efficiency, low price and low toxicity [10, 11].

In order to advance reduce the cost and the inhibitive force, the effect of synergistic inhibition is an efficient technique [12]. This plays a significant role not only in the theoretical research on the corrosion inhibitor but also in the practical work [13].

The synergistic effect increases in the order $I^->Br^->Cl^-$ [14]. The maximum synergistic effect related to bromide ions has been associated with ease of polarizability hence and their large size may be chemisorbed onto steel surfaces [15]. Phenomenon of synergism between bromide and chloride ions was done on corrosion inhibition of carbon steel in acidic environment [16]. Synergistic effect studies of halide ions and polymers in general and bromide ions in individuals have been reported for carbon steel in the literature [17-20]. However, the report about synergistic effect between polyacrylamide in general and tetradecylpyridinium bromide in particular for carbon steel is very rare. Therefore, in this work, the effect of polyacrylamide in general and tetradecylpyridinium bromide on corrosion inhibition of carbon steel rebar in simulated cement-mortar pore solution was studied by electrochemical approaches.

2. MATERIALS AND METHODS

The carbon steel samples have a chemical composition of (wt%): 0.14% C, 0.022% S, 0.36% Mn, 0.057% Si, 0.028% P and Fe balance. These steel rebars had 8 mm diameter and 8 cm length. Before using, chemical cleaning was done on the carbon steel surface. In the simulated cement-mortar pore solutions, its ionic composition principally contains Ca^{2+}, Na^+, OH^- and K^+, and at the early stages of cement hydration, the pH-value of pore solution keeps above 13.0 at 25 ^oC [21]. The calcium leaching produced by water may reduce the pH-value of simulated pore solution to lower than 10.5 [22]. Therefore, in this work, the pH-value of simulated cement-mortar pore solution is calculated as 13.5, and the molar-ratio of $Ca(OH)_2$: NaOH: KOH is 0.001:0.2:0.6 to prepare the pore solution with a pH-value of 13.5. The pH-value of pore solution was adjusted through $NaHCO_3$. $Ca(OH)_2$, NaOH, KOH and $NaHCO_3$ were used as analytical reagents and the purified-water was used as the solvent in this work.

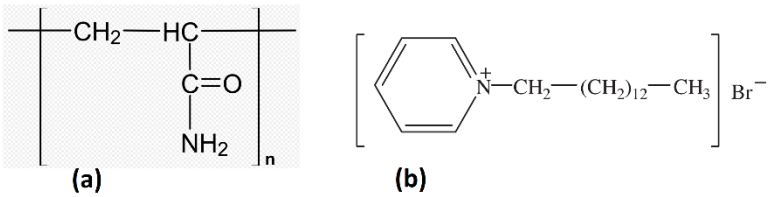

Figure 1. Molecular structures of (a) Polyacrylamide and (b) Tetradecylpyridinium bromide

Polyacrylamide (PA), with the number average molecular weight (M_n) of 3×10^6 g mol^{-1} was used as an inhibitor with a molecular structure which is shown in figure 1a. Tetradecylpyridinium

bromide (TDPB) was used as another inhibitor with the molecular structure which is shown in figure 1b. Both inhibitors were purchased from Shanghai Chemical Reagent Co., Ltd in China. The synergistic inhibition effects were considered with PA and TTAB at mass-ratios of 1:0, 1:0.5, 1:1, 1:2 and 1:4, respectively.

EIS technique was applied to study the corrosion behavior of carbon steel rebars. A triple-electrode system was applied for the measurements which contain the carbon steel bar as the working electrode, a platinum wire and a saturated calomel electrode as an auxiliary and a reference electrode, respectively. The EIS assessments were done at a frequency range from 0.01 Hz to 0.1 MHz after one week immersion time. The analysis was performed after being immersed in a simulated cement-mortar pore solution using a PARSTAT 2273 (Advanced electrochemical system). Inhibition efficiency (η_e) is determined by following equation:

$$\eta_e = \frac{R_{ct} - R_{ct}^*}{R_{ct}} \times 100\% \qquad (1)$$

where R_{ct} and R_{ct}* are charge-transfer resistance values with and without inhibitors, respectively. The polarization analysis was performed from -950 mV to 450 mV at a scan rate of 1mV/s. Inhibition efficiency η_e is determined by following equation:

$$\eta_e = \frac{i_{corr} - i_{corr}^*}{i_{corr}} \times 100\% \qquad (2)$$

where i_{corr} and i_{corr}* show values of corrosion current density with and without inhibitors, respectively. The surface morphologies of the steel rebars were considered by scanning electron microscope (SEM, Zeiss Sigma 300 VP).

3. RESULTS AND DISCUSSION

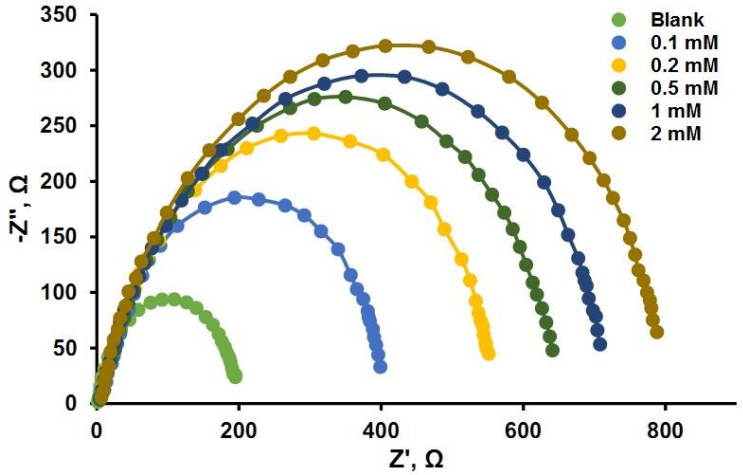

Figure 2. Nyquist diagrams of carbon steels into the simulated cement-mortar pore solution with different concentration of PA inhibitor after one week exposure time

The Nyquist plots of carbon steels into the simulated cement-mortar pore solution with different concentrations of PA inhibitor after one week exposure time are revealed in Fig. 2. As indicated, these plots have similar shape in all tested concentrations which shows that there is almost

no change into the corrosion mechanism with the addition of inhibitors [23]. When the concentration of PA inhibitors enhanced, the diameter of the semi-circle loop enhanced due to the creation of passive layer or adsorption of PA in anodic site of the carbon steel rebar and so reduced the iron dissolution [24]. The passive film reduced the attack of aggressive ions on the surface of the carbon steel rebar and competently controlled the pitting corrosions.

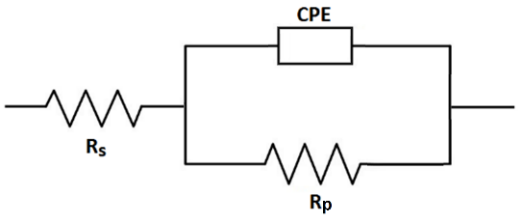

Figure 3. Equivalent circuit model

Figure 3 indicates an equivalent circuit model used in this work. Rs and CPE show the solution resistance and constant phase element. Rp is the polarization resistance which contains diffuse layer resistance (R_d), charge-transfer resistance (R_{ct}), film resistance (R_f) and the resistance of accumulated species in the solution/metal interface (R_a) [25].

$$R_p = R_a + R_{ct} + R_f + R_d \quad (3)$$

The electrochemical parameters of Rp and C_{dl} are determined by ZSimpWin software and revealed in Table 1. As shown, the R_P values were significantly increased from 203 Ω to 811 Ω, as concentration of PA inhibitor increased in the pore solution which indicated that the presence of PA led to the corrosion resistance enhancement of the carbon steel rebar.

Table 1. The electrochemical parameters

PA concentration	R_s (Ω cm^2)	R_p(Ω cm^2)	C_{dl}(μF cm^{-2})
Blank	28	203	79.3
0.1 mM	26	405	74.5
0.2 mM	23	573	63.1
0.5 mM	25	648	52.8
1 mM	27	732	39.2
2 mM	24	811	28.7

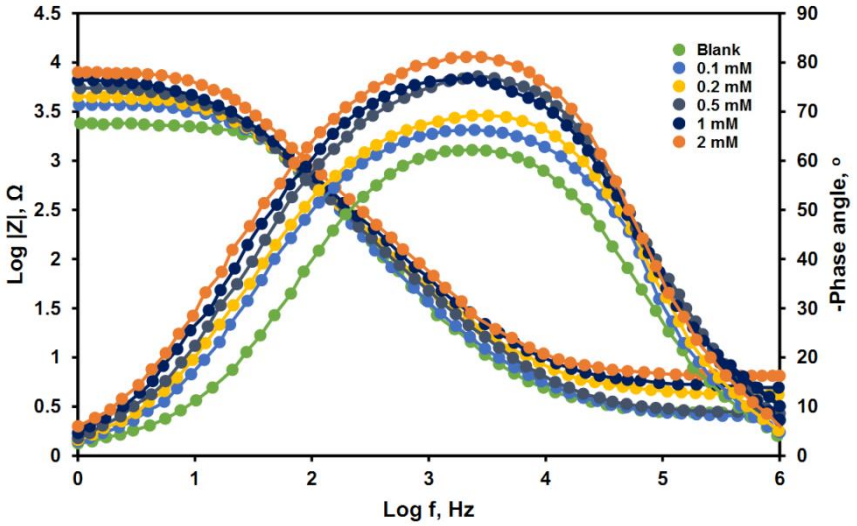

Figure 4. The bode plots of carbon steel rebars immersed in simulated cement-mortar pore solution with different concentration of PA inhibitor after one week exposure time

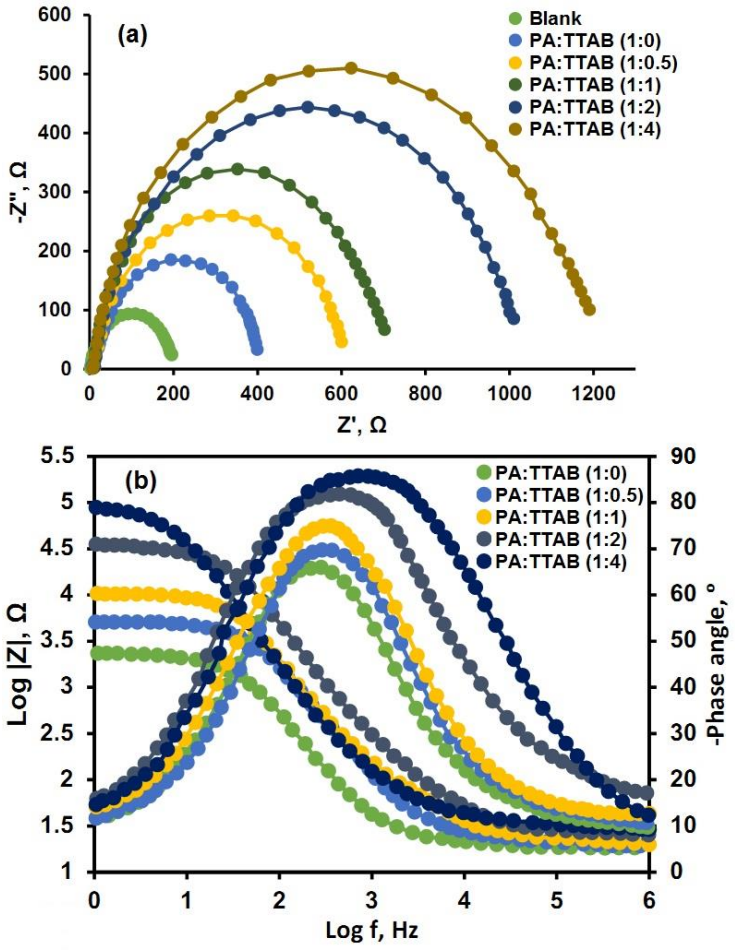

Figure 5. (a) Nyquistand (b) Bode plots of carbon steel rebars immersed in simulated cement-mortar pore solution with different concentration of combined PA and TTAB inhibitors after one week exposure time

Figure 4 indicates the Bode plots of carbon steel rebars immersed in simulated cement-mortar pore solution with different concentrations of PA inhibitor after one week exposure time. As shown, when PA inhibitor contents were increased up to 2 mM, the impedance values increased. This result shows that a high amount of PA inhibitor can strangely control the corrosion behavior of the carbon steel rebars in pore solution. It can be associated with covering the active site on the surface of carbon steel rebar through a PA inhibitor. Moreover, it can be associated with the formation of passive film on carbon steel surfaces by inhibitor adsorption. The sample immersed into the pore solution without PA inhibitor was more sensitive to corrosion due to corrosive ions reached on the surface of carbon steel rebar. Thus, an increase in impedance value was obtained in pore solutions containing PA inhibitors. As revealed in Fig. 4, maximum phase-angle for pore solution containing PA inhibitor was shifted toward a higher angle because of the formation of protective passive film [26]. The phase-angle was shifted from -63° to -82° in pore solutions with blank and 2 mM FA inhibitor, showing the passive film was uniform and homogenous.

In order to evaluate the synergistic effect of TTAB inhibitor on the PA corrosion inhibition for carbon steel rebars in pore solution, EIS measurements were done. Figure 5 shows the Nyquist and Bode plots of carbon steel rebars immersed in simulated cement-mortar pore solution with different concentrations of combined PA and TTAB inhibitors after one week exposure time.

The results obviously reveal a distinct effect of TTAB inhibitor on corrosion behavior of carbon steel compared to blank pore solution without and with PA inhibitor. As shown Figure 5, the semicircle radius in Nyquist plot, maximum phase-angle and impedance of the interface in the Bode plots increase by the addition of TTAB to the PA inhibitor and further increase was found as the concentration of TTAB increases. The Nyquist plots show only one depressed semicircle, which is related to a one-time constant in the Bode diagrams. The capacitive loop can be caused by the time constant of charge-transfer resistance and the electrical double-layer [27]. The increase of the polarization resistance value at low-frequency for the pore solution with PA containing high content of TTAB can be attributed to increased adsorption of bromide ions onto the steel surface which totally displaced adsorbed intermediates or the other species such that the PA inhibitor was now adsorbed on the top of earlier chemisorbed bromide layer and not directly on the surface of carbon steel.

Table 2. The electrochemical parameters

Inhibitor	R_s (Ω cm^2)	R_p(Ω cm^2)	C_{dl}(μF cm^{-2})	$\eta_{e\,(\%)}$
Blank	28	203	79.3	-
PA:TTAB (1:0)	26	405	74.5	49.8
PA:TTAB (1:0.5)	29	604	67.4	66.3
PA:TTAB (1:1)	21	723	62.9	71.9
PA:TTAB (1:2)	23	1046	41.6	80.5
PA:TTAB (1:4)	27	1239	32.7	83.6

The equivalent circuit indicated in Figure 3 was applied to fit the experimental results achieved from the impedance measurements. Table 2 indicates the corresponding electrochemical parameters.

As shown, addition of TTAB to PA inhibitor increased the polarization resistance (Rp) from 203 Ωcm^2 to 1221 Ωcm^2. Moreover, the double-layer capacitance (C_{dl}) reduced by increasing the concentration of TTAB. Inhibition efficiency (η_e) was also observed to be improved from 49.8% for PA to 66.3–83.6% in addition to different concentrations of TTAB to PA pore solution. The enhanced inhibition efficiency arising from the addition of bromide ions to PA inhibitors is because of synergistic effect.

To further evaluate the synergistic effect of PA and TTAB inhibitors on corrosion behavior of carbon steel in simulated cement-mortar pore solution, polarization analysis were done at 40 °C. Figure 6 reveals the polarization plots of carbon steels in the pore solution containing various inhibitors. As shown, the inhibitors may affect both cathodic reactions and anodic dissolution on the surface of carbon steel rebar. The corrosion potential of carbon steel in the existence of inhibitors clearly shifted to the positive direction. The PA and TTAB are mixed-type inhibitors and anodic-type, respectively [28, 29]. Thus, the inhibitors changed from mixed-type to anodic-type through the increase of TTAB concentration, which finally delayed the anodic dissolution of carbon steel. Table 3 indicates the electrochemical parameters obtained from the polarization plots. As indicated in table 3, η_e of PA and TTAB inhibitors is considerably higher than those of only PA. The η_e of the inhibitors increased intensely by increasing TTAB concentration. Although the total η_e values vary from those achieved by the EIS technique, the trends of their change are consistent with the increase of TTAB content achieved by these two techniques.

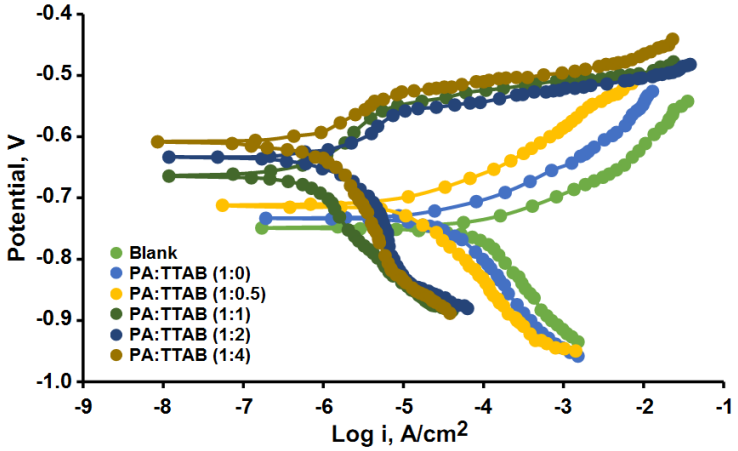

Figure 6. The polarization plots of carbon steels in the pore solution containing various inhibitors

Table 3. The electrochemical parameters obtained from the polarization plots

Inhibitor	E_{corr}(V)	i_{corr}(μA/cm^2)	η_e (%)
Blank	-0.756	151.35	-
PA:TTAB (1:0)	-0.748	91.43	39.6
PA:TTAB (1:0.5)	-0.721	52.62	65.2
PA:TTAB (1:1)	-0.659	1.69	98.8
PA:TTAB (1:2)	-0.627	1.32	99.1
PA:TTAB (1:4)	-0.602	3.46	97.7

From Table 3, it found that the i_{corr} is reduced from 151µA/cm^2 in the blank solution to 91µ/Acm^2 in the existence of PA. The i_{corr} values were further decreased to 52–1.3 µA/cm^2 with the addition of different concentrations of TTAB. Furthermore, inhibition efficiency was improved from 39.6% obtained for only PA to 65–99% in addition to TTAB to PA. This shows the synergistic corrosion effect between TTAB and PA.

Figure 7 indicates the surface morphologies of carbon steel rebar in simulated cement-mortar pore solution with and without inhibitor after one week. Figure 7 presented that the sample exposed to the pore solution containing both PA and TTAB has a more uniform and smooth surface than that one in blank pore solution which confirms previous reports.

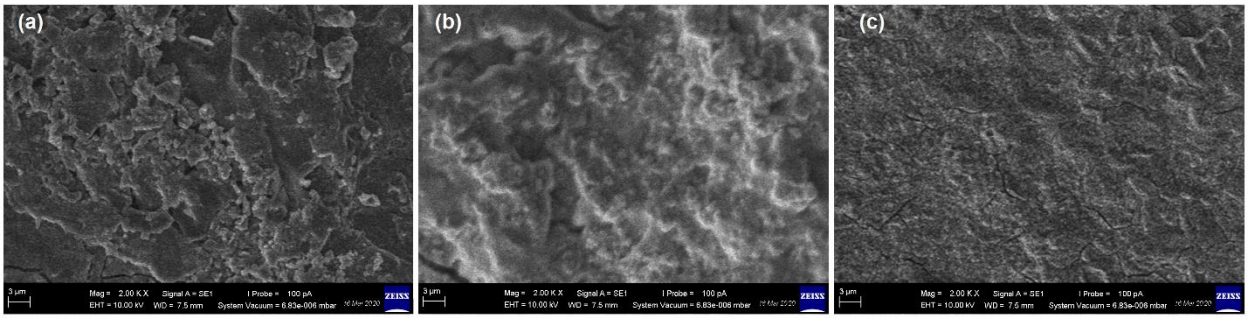

Figure 7. Surface morphologies of carbon steel rebar exposed to (a) blank (b) only PA and (c) PA: TTAB (1:2) pore solution after one week.

4. CONCLUSIONS

Using inhibitors is one of most practical techniques for protecting metals against corrosion, particularly in an alkaline environment. In this research, synergistic inhibition effect of PA and TTAB on the corrosion behavior of carbon steel rebar in simulated cement-mortar pore solution was evaluated by EIS and potentiodynamic polarization techniques. The EIS results revealed that the PA as a mixed-type inhibitor considerably enhanced corrosion protection performance in carbon steel rebar with creation of an organic layer to prevent both cathodic and anodic corrosion reactions. The obtained electrochemical results show that the inhibition efficiency of PA was significantly enhanced in the presence of TTAB for carbon steel rebar which confirms the synergistic corrosion effect between TTAB and PA. Because the inhibitor type changed from mixed-type to anodic-type through the increase of TTAB concentration, they eventually delayed the anodic dissolution of carbon steel which reduced the corrosion rate of the steel rebar in an aggressive environment. FESEM results indicated that the carbon steel rebars exposed to the pore solution containing both PA and TTAB had a more uniform and smooth surface than that one in blank pore solution.

ACKNOWLEDGEMENT
This work was supported by the National Natural Science Foundation of China (No. 11862024). These authors contributed equally to this work and should be considered co-first authors.

References

1. B.D. Choudhury, C. Lin, S.M.A.Z. Shawon, J. Soliz-Martinez, J. Gutierrez, M.N. Huda, F. Cesano, K. Lozano, J.Z. Zhang and M.J. Uddin, *ACS Applied Energy Materials*, 4 (2021) 870.
2. K. Yu, L. Li, J. Yu, J. Xiao, J. Ye and Y. Wang, *Engineering Structures*, 170 (2018) 11.
3. S. Kakooei, H.M. Akil, A. Dolati and J. Rouhi, *Construction and Building Materials*, 35 (2012) 564.
4. A. Zhou, C.L. Chow and D. Lau, *Composites Part B: Engineering*, 136 (2018) 1.
5. M. Askari, M. Aliofkhazraei, S. Ghaffari and A. Hajizadeh, *Journal of Natural Gas Science and Engineering*, 58 (2018) 92.
6. S. Kakooei, H.M. Akil, M. Jamshidi and J. Rouhi, *Construction and Building Materials*, 27 (2012) 73.
7. K.W. Shinato, A.A. Zewde and Y. Jin, *Corrosion Reviews*, 38 (2020) 101.
8. D. Liu, Y. Song, D. Sha and E.H. Han, *International Journal of Electrochemical Science*, 13 (2018) 2219.
9. C. Verma, L. Olasunkanmi, E.E. Ebenso and M. Quraishi, *Journal of Molecular Liquids*, 251 (2018) 100.
10. D. Zhang, J. Liu, P. Li, Z. Tian and C. Liang, *ChemNanoMat*, 3 (2017) 512.
11. S. Wang, Y. Zuo, Y. Tang and X. Zhao, *International Journal of Electrochemical Science*, 13 (2018) 842.
12. X. Li and S. Deng, *Journal of Materials Research and Technology*, 9 (2020) 15604.
13. Z. Hajiahmadi and Z. Tavangar, *Journal of Molecular Liquids*, 284 (2019) 225.
14. M. Saleh, M.G. Mahmoud and H.M. Abd El-Lateef, *Corrosion Science*, 154 (2019) 70.
15. S.K. Ahmed, W.B. Ali and A.A. Khadom, *International Journal of Industrial Chemistry*, 10 (2019) 159.
16. Z. Yang, C. Qian, W. Chen, M. Ding, Y. Wang, F. Zhan and M.U. Tahir, *Colloid and Interface Science Communications*, 34 (2020) 100228.
17. M. Mobin, R. Aslam and J. Aslam, *Materials Chemistry and Physics*, 223 (2019) 623.
18. A.L. Chong, J.I. Mardel, D.R. MacFarlane, M. Forsyth and A.E. Somers, *ACS Sustainable Chemistry & Engineering*, 4 (2016) 1746.
19. M. Djellab, H. Bentrah, A. Chala and H. Taoui, *Materials and Corrosion*, 70 (2019) 149.
20. B. Zhang, C. He, X. Chen, Z. Tian and F. Li, *Corrosion Science*, 90 (2015) 585.
21. A. Behnood, K. Van Tittelboom and N. De Belie, *Construction and Building Materials*, 105 (2016) 176.
22. M. Moranville, S. Kamali and E. Guillon, *Cement and Concrete Research*, 34 (2004) 1569.
23. M. Veloz and I. Gonzalez, *Electrochimica acta*, 48 (2002) 135.
24. A. Fouda, G. Elewady, K. Shalabi and H.A. El-Aziz, *RSC Advances*, 5 (2015) 36957.
25. J. Rouhi, S. Kakooei, M.C. Ismail, R. Karimzadeh and M.R. Mahmood, *International Journal of Electrochemical Science*, 12 (2017) 9933.
26. H.-S. Ryu, J.K. Singh, H.-S. Lee, M.A. Ismail and W.-J. Park, *Construction and Building Materials*, 133 (2017) 387.
27. M. Morad and A. Sarhan, *Corrosion Science*, 50 (2008) 744.
28. S. Umoren, Y. Li and F. Wang, *Corrosion Science*, 52 (2010) 1777.
29. A. Singh, Y. Lin, I. Obot and E.E. Ebenso, *Journal of Molecular Liquids*, 219 (2016) 865.